3D Freehand Ultrasound for Medical Assistance in Diagnosis and Treatment of Breast Cancer: Preliminary Results

[a]Fabian Torres, [b]Zian Fanti, F. Arámbula Cosío
[a]PhD Program in Electrical Engineering and Digital Signal Processing, UNAM
[b]PhD Program in Computer Science and Engineering, UNAM
Biomedical Imaging Lab.,
Center of Applied Science and Technological Development,
Universidad Nacional Autónoma de México (UNAM),
México, D.F., 04510.

ABSTRACT

Image-guided interventions allow the physician to have a better planning and visualization of a procedure. 3D freehand ultrasound is a non-invasive and low-cost imaging tool that can be used to assist medical procedures. This tool can be used in the diagnosis and treatment of breast cancer. There are common medical practices that involve large needles to obtain an accurate diagnosis and treatment of breast cancer. In this study we propose the use of 3D freehand ultrasound for planning and guiding such procedures as core needle biopsy and radiofrequency ablation. The proposed system will help the physician to identify the lesion area, using image-processing techniques in the 3D freehand ultrasound images, and guide the needle to this area using the information of position and orientation of the surgical tools. We think that this system can upgrade the accuracy and efficiency of these procedures.

Keywords: Breast cancer, 3D freehand ultrasound, core needle biopsy, image segmentation.

1. INTRODUCTION

Ultrasound has become a useful tool for assisting medical diagnosis and procedures, because it has some advantages over other imaging modalities such as magnetic resonance (MR) or computed tomography (CT). Ultrasound is a minimal invasion and low-cost imaging modality; it also has the ability to obtain real time images of a wide area of the patient anatomy in several directions[1].

Breast cancer is one of the leading causes of death in women all around the world, so an early and accurate diagnosis is crucial for a successful treatment[2]. Ultrasound has been used as one of the gold standards for breast cancer imaging, since physicians are able to visualize in real time some characteristics of the tumor that may differentiate it as malignant or benign[3]. However, the most accurate method for breast cancer diagnosis is the biopsy[4], with a sensitivity of 92% when the tumor has a size between 1.8 and 3cm[5]. Because of this, ultrasound-guided needle biopsy has become a common practice to obtain an accurate diagnosis of breast cancer; in fact, the National Institute for Clinical Excellence of United Kingdom recommends the use of ultrasound in all selective line needle insertions[6]. Although this procedure has become a gold standard for breast cancer diagnosis, the use of conventional 2D ultrasound may have some disadvantages; because of inherent artifacts of ultrasound images, such as speckle, acoustic shadows and blurry boundaries, some lesions can have low contrast with the healthy tissue and the visualization may be poor[7]; choosing the visualization plane of the lesion may be a difficult task[8]; aligning the needle with the visualization plane its also a difficult task and the visualization of the needle may be poor[9].

There exist some other medical procedures that use conventional ultrasound for the diagnosis and treatment of breast cancer. Radiofrequency ablation is a treatment method that consists of introducing a needle electrode that radiates the lesion area with electric currents to destruct malignant cells by heating them[10]. Ultrasound can be used to guide and monitor the procedure[11]. On the other hand, elastography is a diagnosis method, based on ultrasound images, that can obtain mechanical properties of the tissue[12] . Elastography has been used in the examination of breast lesions for the purpose of differentiating from benign and malignant tumors[13]. However, as in ultrasound-guided needle biopsy, the use of conventional 2D ultrasound may lead to some disadvantages.

The use of image processing techniques and 3D ultrasound may be able to reduce some of these disadvantages and upgrade the accuracy and efficiency of these procedures. In this paper we propose a system that can help the physician to

plan, guide and monitor these procedures by using 3D freehand ultrasound, tracked instruments and semi-automatic segmentation techniques for breast tumors in ultrasound images. We think that the information obtained from 3D ultrasound and image segmentation is sufficient to create a deformable model of the patient anatomy, allowing the physician to obtain pre-operative and intra-operative images in the same session, without transferring the patient form a one room to another and without using invasive and high-cost imaging methods like CT or MR. The organization of the paper is as follows. In section 2, we discuss the previous work. In section 3, we present the implementation of the used methods. In section 4, we present our preliminary results. Finally, in section 5 we present our conclusions and a discussion of future work.

2. PREVIOUS WORK

2.1 3D freehand ultrasound

The usage of 3D ultrasound for planning and guiding medical procedures, as the ones mentioned before, may reduce some disadvantages, giving the physician the opportunity to have a complete visualization of the lesion in any direction. 3D freehand ultrasound is a technique to obtain ultrasound volumes using conventional 2D ultrasound probes. It has some advantages over other 3D ultrasound techniques (mechanical 3D ultrasound and 2D array probes); it is a low-cost technique and the size of the volume is not limited by the size of the probe[14]. Most of the 3D freehand ultrasound systems consist of a 2D conventional ultrasound system and a position and orientation tracker mounted over the probe[15].

Most of the 3D freehand methods for obtaining an ultrasound volume consist of three steps. First a probe calibration has to be done; after calibrating the system, the acquisition of the images and their tracked position takes place; finally, a volume reconstruction algorithm generates the ultrasound volume using the previously acquired data. The probe calibration consists of obtaining the transformation matrix ${}^{S}T_{I}$ that relates the coordinate system of the image plane (I) with the sensor coordinate system (S) as shown in figure 1. Prager, *et al.*[16] and later Hsu, *et al.*[17] made a comparison of several calibration methods and demonstrate that the single point calibration methods are the best, because of the easy construction of the used phantom and small reconstruction error. After calibrating the probe it is possible to acquire the 2D ultrasound images and their position and orientation obtained using the data acquired from the tracker and the transformation matrix obtained in the calibration. The reconstruction process consists of filling a voxel array by interpolating the information of the 2D images and their positions and orientations. There are several volume reconstruction techniques, Solberg *et al.*[18] compare some techniques and demonstrate some advantages and some disadvantages in those techniques. In the volume reconstruction process exist some considerations to take into account (such as size, position and orientation of the volume, and the size of the voxel) that may affect the time and quality of the reconstruction.

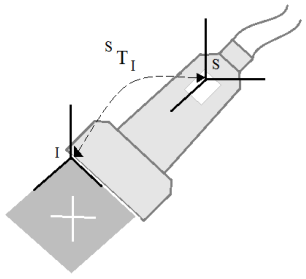

Figure 1. Calibration Process. Shows the matrix STI that relates the coordinate system I and S.

2.2 Breast tumor segmentation in ultrasound images

The visualization of breast tumors in ultrasound images may be a difficult task for inexperience users, because of inherent artifacts of the ultrasound images. A good segmentation method may be able to help the physician to have a better visualization of the lesion, but it is not an easy image-processing task[7]. The main artifacts that make segmentation of breast tumors in ultrasound images a challenging task are speckle, acoustic shadows, blurry boundaries and shape of the tumors[19]; also there are some healthy tissues that may look like tumors in ultrasound images[20].

There are several works related with the segmentation of breast tumors in ultrasound images. Most of these works consist on a pre-processing step and a segmentation step. The pre-processing step consists in filtering and contrast

enhancement of the image. Some works have used Gaussian[7] and Butterworth[20] filters , but it has been probe by Abd *et al*.[21] that the Gaussian anisotropic filter, as the one used in Chang *et al*.[19], have good results in ultrasound images. The contrast enhancement of the image has been carried away with sticks method[3,7,19] and with histogram equalization[20]. The segmentation step can be divided in two groups, thresholding based methods and classifiers based methods. The formers are low computational cost and use the gray-level intensity of the pixels to segment the image[7,19,22]; however, these methods are not able to differentiate acoustic shadows from tumors. The latter group use classifiers to segment the images[2,3,20,23], these are more robust since they use more than one characteristic for classifying the pixels as tumor or healthy tissue; however these are more difficult to implement and the computational cost increments considerably. A good segmentation method must take in account the spatial position, the texture and the intensity of the lesion[20].

2.3 Breast tumor biopsies and 3D elastography

Ultrasound-guided biopsy is a method than helps the physician to obtain a small sample of tissue by guiding a core needle to the lesion; however, as mentioned before, this method has some disadvantages. Several works have been carried on to upgrade the accuracy of stereotactic and ultrasound-guided biopsies. Azar *et al*.[24] propose the use of a deformable model obtained from a magnetic resonance to plan a stereotactic biopsy. Fenster *et al*.[25] propose a system that uses the advantages of mechanical 3D ultrasound and stereotactic biopsy. Other works use tracked instruments and virtual reality to guide the procedure[4,26]. Most of the works based on deformable models obtain the tissue information from segmented images of MR or CT. One important problem to take into account while taking a biopsy is the tissue displacement due to the interaction of surgical tools with it. During needle insertion, the forces involved tend to push the tissue away from the needle[27], none of these papers take into account this problem, only Fenster *et* al.[25] use 3D ultrasound to check if the needle was inserted in the proper place. This problem requires a new generation of systems based on adaptive 3D images[28]. We think that 3D freehand ultrasound with deformable models may be a good solution for this problem.

The main problem with conventional elastography is to choose the correct image plane and to apply a non-uniform stress field[13]. Mechanical probes have been used to assist the physician in this procedure to obtain better strain images[29]. Another approach to obtain better images is the use of 3D ultrasound, Deprez *et al*.[12] use a mechanical probe, while Lindop *et al*.[30] use 3D freehand ultrasound to obtain the 3D elastography. We think an adaptive image obtained with 3D freehand ultrasound and deformable models can be used to obtain a good approximation of the 3D deformation of the tissue and with that information obtain a 3D elastography.

3. METHODOLOGY

In this section we present the methodology and the implemented methods for the proposed system. In figure 2 we show a block diagram of the methodology for planning and guiding a breast tumor biopsy, latter we explain the already implemented methods (highlighted in gray in figure 2).

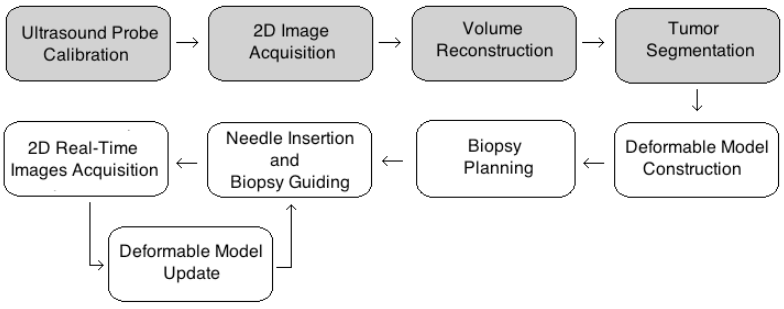

Figure 2. Block diagram for the proposed system for planning and guiding breast tumor biopsies.

The implementation of the methods was made in C++ in a MacPro with an Intel Xenon of 2.83GHz processor with 3GB in RAM and Mac OSX 10.6 64bits operating system, using free-access libraries for the processing and visualization of the images. The used libraries are ITK, VTK and IGSTK; these libraries are property of Kitware Inc (http://www.kitware.com). For image acquisition an Aloka SSD-1000 ultrasound system with a 2D probe at 7.5Mhz is

used with a CyberOptics Semiconductor PXR800 acquisition card. For tool tracking a passive optical tracker Polaris Spectra of Nothern Digital is used.

3.1 3D freehand ultrasound

To calibrate the ultrasound probe we implement the cross-wire method described by Prager *et al*.[16]. It consists in two wires that cross in one point submerged on water. Several images of the cross-wire point are taken in several positions and orientations, and a manual segmentation of the cross-wire point is made in each image; with this data a system of nonlinear equations can be generated and solved to obtain the eight parameters involved in the calibration process, three for translation (x, y and z), three for rotation (α, β and γ) and two for scale (e_x and e_y). For solving the system we use a free-access library that implements the Levenberg-Marquardt algorithm[31]. The transformation matrices T, which have the form of a translation and rotation matrix (equation 1), involved in the calibration method are shown in figure 3. The relation between these matrices, to obtain the nonlinear equations is shown in equation 2; where I is the image coordinate system, S is the sensor coordinate system, T is the tracker coordinate system and H is the cross-wire coordinate system.

$$ {}^{J}T_{I}(x,y,z,a,b,g)=\begin{bmatrix} \text{cosacosb} & \text{cosasinbsing-sinacosg} & \text{cosasinbcosg+sinasing} & \text{x} \\ \text{sinacosb} & \text{sinasinbsing+cosacosg} & \text{sinasinbcosg+cosasing} & \text{y} \\ \text{-sinb} & \text{cosbsing} & \text{cosbcosg} & \text{z} \\ 0 & 0 & 0 & 1 \end{bmatrix} \tag{1} $$

$$ \begin{bmatrix} 0 \\ 0 \\ 0 \\ 0 \end{bmatrix} = {}^{H}T_{R}\,{}^{R}T_{S}\,{}^{S}T_{I} \begin{bmatrix} e_x u \\ e_y v \\ 0 \\ 1 \end{bmatrix} \tag{2} $$

To make a volume reconstruction we implement a trilinear interpolation algorithm proposed by Trobaugh *et al*.[32]. This algorithm makes an interpolation from the two nearest surrounding image planes. It traverses all the voxels and calculates a normal to each of these image planes and the four surrounding pixels are bilinearly interpolated in each plane. The gray value of the voxel is calculated as the weighted sum with contribution of the two planes based on the distance from the voxel to the planes[18]. Figure 4 shows a diagram that explains the reconstruction method.

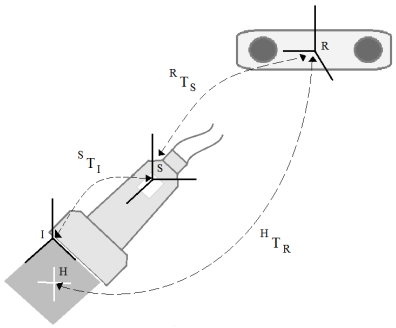

Figure 3. Coordinate systems involved during the calibration process and the transformations T that relate them.

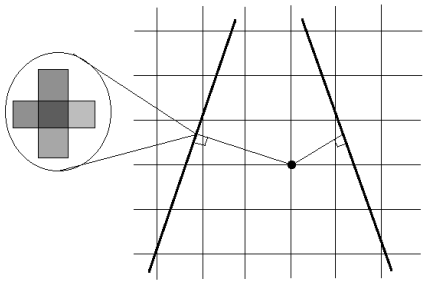

Figure 4. Throbaugh *et al*. reconstruction method diagram.

The volume size and position where taken from the images position and orientation data, while the voxel size is equal to the size of the image pixel by a constant *k*, where *k* can have any value between 1 and 10; the smaller the value of *k*, we will be able to reconstruct smaller objects, but the processing time will be higher.

3.2 Breast tumor segmentation

A similar method to the one proposed by Madabushi *et al.*[20] was implemented for breast tumor segmentation in ultrasound images. The method consists in segmenting a probability image instead of an intensity image. The probability image refers to the representation of the probability of each pixel to belong to the tumor with respect to its intensity and its texture. To obtain this probability, *a priori* information is needed to obtain the intensity and texture probability density function (PDF). We use 30 previously manual segmented images to obtain the PDFs. With these PDFs we can obtain the joint probability of each pixel to belong to the tumor with respect to its intensity and texture. These PDFs are shown in figure 5, where the probability of belonging to healthy tissue is only shown to demonstrate that it is possible to differentiate the tumor region from the healthy tissue using probabilities.

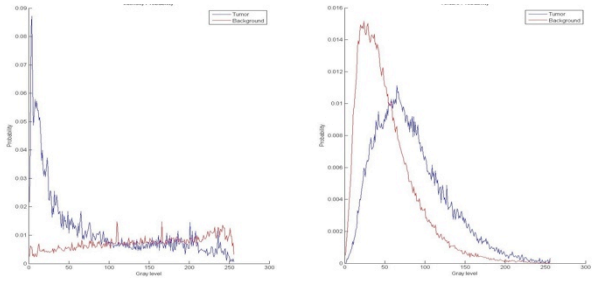

a) b)

Figure 5. a) Intensity probability and b) texture probability. In blue the probability to belong to a tumor and in red the probability to belong to healthy tissue.

To obtain an intensity image we use a pre-processing step that consists of a contrast enhancement and filtering of the original image. The contrast enhancement was carried on by a histogram equalization to accentuate the edges of the objects in the image and an anisotropic Gaussian filter was used to homogenize the regions without blurring the enhanced edges.

Texture analysis in ultrasound images is not an easy task. First-order descriptors like the one used by Madabushi *et al.*[20] are not able to give a good texture description of ultrasound images, because they do not take into account the spatial relationship between pixels[33]. Based on the studies of Liao, *et al.*[34] and Chen *et al.*[35], we use the variance of the co-occurrence matrix as the texture descriptor. For this we obtain four co-occurrence matrices, one in each direction θ (where θ=0º, 45º, 90º and 135º) and obtain the variance of the mean co-occurrence matrix. A pre-processing step to obtain the texture image is not used to avoid the elimination of relevant information.

Once the intensity and texture images are obtained, we can use the PDFs to obtain a probability image that would have a high contrast between the tumor and the healthy tissue. To obtain the region that belongs to the tumor a region growing method is used. While in the work of Madabushi *et al.*[20] the seed of the region is chosen automatically, we decide to choose the region seed manually, allowing the physician to choose between high probability regions according to the space localization of the tumor and his expert knowledge. The region growing conditions are shown in equation 3[20].

$$t \in T \Leftrightarrow \beta_1 J_{C_0} \leq I_p(t) \leq \beta_2 J_{C_0} \; and \; T \cap N_t(t) \neq 0 \tag{3}$$

where t is any pixel and T is the tumor region. The first expression ($\beta_1 J_{C_0} \leq I_p(t) \leq \beta_2 J_{C_0}$) implies that the value of t in the probability image I_p is in between a range of values that depends on the mean value of the seed neighborhood J_{C_0} and the threshold values β_1 and β_2; while the second expression ($T \cap N_t(t) \neq 0$) implies that the neighborhood of the pixel t intersects with the tumor region.

The tumor edges found with the region growing method can later be used as an initialization for a deformable model like Snakes to propagate the 2D segmentation to the 3D volume like in[7].

4. RESULTS

In this section we present the partial results for the calibration, reconstruction and segmentation method. For the calibration and reconstruction methods we use *in-vitro* validation methods and for the segmentation we use real ultrasound images of breast tumors obtained from a private image database provided by the National Taiwan University.

4.1 Calibration

Unfortunately, there is no standard method to validate the accuracy of a calibration. The method we use for validating our calibration consists of acquiring several images of a tracked sphere and segmenting several points over the sphere borders manually in each image to obtain an estimated sphere that best fits the segmented points. The accuracy error is reported as the distance between the tracked sphere and the estimated sphere. For evaluating a calibration, obtained with 50 cross-wire images, we use one tracked sphere and acquire 10 images of it and segment 2400 point over the surface; the accuracy error obtained in this calibration was 0.556mm.

Another important calibration error that should be measure is calibration precision. This is the error committed by transforming a single point in different image planes. To obtain this error we acquire several images in different planes of one point. After reconstructing the point in each image, we obtain the absolute standard deviation of the point cloud and report this as the precision error. For the previously mentioned calibration we obtain a precision error of 0.249mm.

4.2 Reconstruction

For evaluating the reconstruction error of the implemented algorithm we use an ultrasound phantom (Ultrasound Resolution Phantom Model 044, CIRS) that has tree groups of cylinders. The first group consists of six cylinders of 1.5mm, the second group consists of nine cylinders of 3mm and the third group consists of two cylinders of 12mm. Five reconstructions of each group were made with different voxel size (k = 1, 3, 5, 8 and10). The diameter of the cylinders in each reconstruction was manually segmented by two different users; the mean measurements for each group of cylinders and voxel size are reported in table 1.

Although the processing time depends on the size of the voxel and the number of 2D images, we where able to reconstruct cylinders with 1.5mm using k = 8 and 81 images, in less than 1 minute with a reconstruction error of 0.22mm.

Table 1. Measurements of the cylinders in the ultrasound phantom in millimeters; X: Horizontal diameter, Y: Vertical Diameter, --: Not able to measure.

	Group 1		Group 2		Group 3	
k	X	Y	X	Y	X	Y
10	12.87	12.86	3.25	2.91	--	--
8	13.10	13.35	3.15	3.16	1.77	1.70
5	12.7	12.8	3.14	3.06	1.73	1.65
3	12.9	13.15	3.32	3.05	1.66	1.43
1	12.5	12.7	3.21	3.03	1.69	1.64

4.3 Segmentation

In figure 6 we present the results of obtaining the probability image of two ultrasound images, one that doesn't contain acoustic shadows and one that contains acoustic shadows bellow the tumor; figure 6a and 6b respectively. In this figure we can see that the intensity probability image (second column) is not able to get rid of the acoustic shadows bellow the tumor, because these present gray intensity values similar to the ones found inside the tumor, and the texture probability image (third column) is able to increase the intensity value of the tumor edges. We observe in the fourth column of figure 5, that the joint probability image has a high contrast between the tumor and the healthy tissue; it is also shown in figure 5b that the joint probability image gets rid of the acoustic shadows below the tumor.

The region growing results are shown in figure 7a and 7b for both probability images in figure 6. The first column corresponds to the original image; the second column corresponds to the region that belongs to the tumor; while the third column shows the tumor edges overlapped in the original image. It is important to mention that the result of the region growing method may vary significantly depending on the position of the seed.

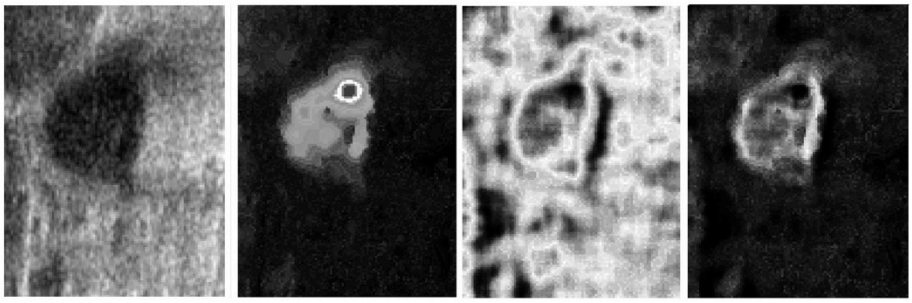

a)

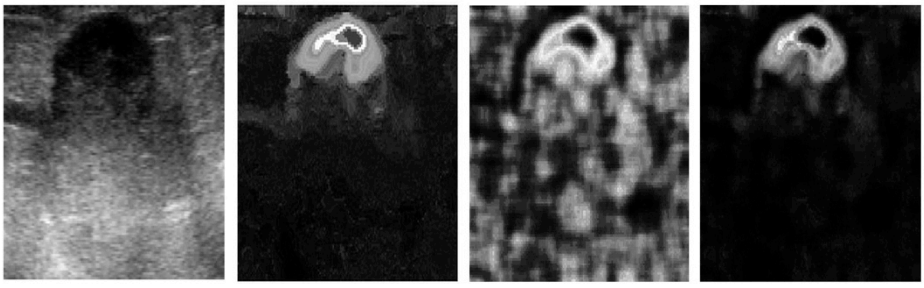

b)

Figure 6. Probability image process. a) Image without acoustic shadows. b) Image with acoustic shadows; Original image in first column; Intensity probability image in second column; Texture probability image in third column; Joint probability image in fourth column.

a)

b)

Figure 7. Region growing process. a) Image without acoustic shadows. b) Image with shadows; Original image in first column; Tumor region in second column; Overlapped tumor edges on the original image in third column.

5. CONCLUSIONS AND DISCUSSION

In this paper we present some methods that could assist the physician in planning and guiding a biopsy of breast tumors using 3D freehand ultrasound and image processing methods. The obtained calibration and reconstruction errors are sufficiently small for the proposed applications, since these are only fractions of millimeters. However it is important to mention that the calibration accuracy was only tested in one sphere; to have more reliable information of the accuracy of the calibration it would be important to check the error with more spheres in different positions. The reconstructions error shows that even with low resolutions ($k > 5$) we were able to reconstruct the cylinders with less than 10% of deformation in X and Y directions.

In a qualitative study, we see that the segmentation method is capable of segmenting the tumor region and differentiate it from acoustic shadows with sufficient accuracy for these applications; since it is not necessary that the segmentation method find the tumor boundaries with great accuracy, because we are targeting the center of the tumor region for needle placement. However it would be important to have a quantitative study that could give us the exact accuracy of our segmentation method; proper validation is being carried on. The segmentation results may vary depending on the seed position, the seed must be a representative point of the tumor, this is the reason why we leave this decision to the expert, who according to his knowledge may be able to choose a correct point. If the region growing results are not satisfactory, the seed position can be updated easily.

These methods could help the physician to have a better understanding of the 3D anatomy of each patient and the position of the tumor within it. The shown methods for 3D freehand ultrasound and tumor segmentation in breast ultrasound images can be used, with the tracked surgical instruments, to create a virtual environment to assist the physician like the one created by Arámbula *et al*[26]. Although the presented methods can be helpful, it is important to take into account tissue displacement due to the interaction with the needle, the creation of new methods to obtain adaptive images is needed[28]. One disadvantage of 3D freehand ultrasound is that it generates static images; however, with the information of the segmented volume we could be able to generate a deformable model of the patient anatomy that can be updated with real-time information acquired from the conventional 2D ultrasound probe during needle insertion. Similar works have been made by Lunn *et al*.[36] using information from segmented MRI and 2D ultrasound to assist neurosurgeries. It is not of our knowledge that a system like the one proposed here has been made, since it uses only freehand ultrasound and a tracker to obtain the needed information. The most similar work to this one, is the one proposed by Nakamoto *et al*.[37] for guiding a liver laparoscopy surgery; however, they use a mechanical 3D ultrasound probe and do not use real-time information to update the 3D ultrasound volume during the surgery.

This system could be used in other needle involving procedures like radiofrequency ablation. It also, may be useful in other procedures that involve tissue displacement like elastography, the deformable model obtained with the system may be useful to estimate 3D deformations of a tumor while applying forces of compression.

ACKNOWLEDMENTS

The authors would like to thank the National Institute of Science and Technology of Mexico City and the National Autonomous University of Mexico for the support of this work.

REFERENCES

[1] Halliwell M. A tutorial on ultrasonic physics and imaging techniques. *Proceedings of the Institution of Mechanical Engineers, Part H: Journal of Engineering in Medicine*. 2010;224(2):127–142.

[2] Jiao J, Wang Y. Automatic boundary detection in breast ultrasound images based on improved pulse coupled neural network and active contour model. In: *5th International Conference on Bioinformatics and Biomedical Engineering, iCBBE 2011*.; 2011.

[3] Huang Q-H, Lee S-Y, Liu L-Z, Lu M-H, Jin L-W, Li A-H. A robust graph-based segmentation method for breast tumors in ultrasound images. *Ultrasonics*. 2012;52(2):266–275.

[4] Badawi AM, El-Mahdy MA. Path planning simulation for 3D ultrasound guided needle biopsy system. *Circuits and Systems, 2003 IEEE 46th Midwest Symposium on*. 2003;1:345–347.

[5] Luechakiesttisak P, Rungkaew P. Breast Biopsy: Accurcy of Core Needle Biopsy Compared with Excisional or Incisional Biopsy: A Prospective Study. *Thai Journal of Surgery*. 2008;29:6–14.
[6] Magee D, Zhu Y, Ratnalingam R, Gardner P, Kessel D. An augmented reality simulator for ultrasound guided needle placement training. *Medical and Biological Engineering and Computing*. 2007;45(10):957–967.
[7] Chen D-R, Chang R-F, Wu W-J, Moon WK, Wu W-L. 3-D breast ultrasound segmentation using active contour model. *Ultrasound in Medicine and Biology*. 2003;29(7):1017–1026.
[8] Goksel O, Salcudean SE. B-Mode Ultrasound Image Simulation in Deformable 3-D Medium. *IEEE Transactions on Medical Imaging,*. 2009;28:1657–1669.
[9] Youk JH, Kim EK, Kim MJ, Lee JY, Oh KK. Missed breast cancers at US-guided core needle biopsy: how to reduce them. *Radiographics*. 2007;27(1):79–94.
[10] Illing R, Gillams A. Radiofrequency Ablation in the Treatment of Breast Cancer Liver Metastases. *Clinical Oncology*. 2010;22(9):781–784.
[11] Hayashi AH, Silver SF, van der Westhuizen NG, et al. Treatment of invasive breast carcinoma with ultrasound-guided radiofrequency ablation. *The American Journal of Surgery*. 2003;185(5):429–435.
[12] Deprez JF, Cloutier G, Schmitt C, et al. 3D ultrasound elastography for early detection of lesions. evaluation on a pressure ulcer mimicking phantom. *Conference proceedings : ... Annual International Conference of the IEEE Engineering in Medicine and Biology Society. IEEE Engineering in Medicine and Biology Society. Conference*. 2007;2007:79–82.
[13] Yen P-L, Chen D-R, Yeh K-T, Chu P-Y. Development of a stiffness measurement accessory for ultrasound in breast cancer diagnosis. *Medical Engineering and Physics*. 2011;33(9):1108–1119.
[14] Fenster A, Downey DB. 3-D ultrasound imaging: A review. *Engineering in Medicine and Biology Magazine, IEEE*. 1996;15(6):41–51.
[15] Berg S, Torp H, Martens D, et al. Dynamic three-dimensional freehand echocardiography using raw digital ultrasound data. *Ultrasound in Medicine and Biology*. 1999;25(5):745–753.
[16] Prager RW, Rohling RN, Gee AH, Berman L. Rapid calibration for 3-D freehand ultrasound. *Ultrasound in Medicine and Biology*. 1998;24(6):855–869.
[17] Hsu P-W, Prager R, Gee A, Treece G. Freehand 3D Ultrasound Calibration: A Review. In: Sensen C, Hallgrímsson B, eds. *Advanced Imaging in Biology and Medicine*. Springer Berlin Heidelberg; 2009:47–84.
[18] Solberg OV, Lindseth F, Torp H, Blake RE, Hernes TAN. Freehand 3D Ultrasound Reconstruction Algorithms—A Review. *Ultrasound in Medicine & Biology*. 2007;33(7):991–1009.
[19] Chang R-F, Wu W-J, Moon WK, Chen D-R. Automatic ultrasound segmentation and morphology based diagnosis of solid breast tumors. *Breast Cancer Research and Treatment*. 2005;89(2):179–185.
[20] Madabhushi A, Metaxas DN. Combining low-, high-level and empirical domain knowledge for automated segmentation of ultrasonic breast lesions. *IEEE Transactions on Medical Imaging*. 2003;22(2):155–169.
[21] Abd-Elmoniem KZ, Youssef A-BM, Kadah YM. Real-time speckle reduction and coherence enhancement in ultrasound imaging via nonlinear anisotropic diffusion. *IEEE Transactions on Biomedical Engineering*. 2002;49(9):997–1014.
[22] Huang S-F, Chen Y-C, Woo KM. Neural network analysis applied to tumor segmentation on 3D breast ultrasound images. In: *2008 5th IEEE International Symposium on Biomedical Imaging: From Nano to Macro, Proceedings, ISBI.*; 2008:1303–1306.
[23] Liu B, Cheng HD, Huang J, Tian J, Tang X, Liu J. Fully automatic and segmentation-robust classification of breast tumors based on local texture analysis of ultrasound images. *Pattern Recognition*. 2010;43(1):280–298.
[24] Azar FS, Metaxas DN, Schnall MD. Methods for Modeling and Predicting Mechanical Deformations of the Breast under External Perturbations. *Handbook of Numerical Analysis*. 2004;12:591–656.
[25] Fenster A, Surry KJM, Mills GR, Downey DB. 3D ultrasound guided breast biopsy system. *Ultrasonics*. 2004;42(1-9):769–774.
[26] Arámbula Cosío F., Hevia N, Lira E, et al. Mammographic image analysis and computer assisted biopsy of breast tumors. In: *Biomedical Engineering and Informatics (BMEI), 2011 4th International Conference on*.Vol 1.; 2011:360–364.
[27] Ayvaci A, Yan P, Xu S, Soatto S, Kruecker J. Biopsy needle detection in transrectal ultrasound. *Computerized Medical Imaging and Graphics*. 2011;35(7–8):653–659. Available at: http://www.sciencedirect.com/science/article/pii/S0895611111000620.

[28] Platenik LA, Miga MI, Roberts DW, et al. In vivo quantification of retraction deformation modeling for updated image-guidance during neurosurgery. *IEEE Transactions on Biomedical Engineering*. 2002;49(8):823–835.
[29] Kadour MJ, Noble JA. Assisted-freehand ultrasound elasticity imaging. *IEEE Transactions on Ultrasonics, Ferroelectrics, and Frequency Control*. 2009;56(1):36–43. 60349091543&partnerID=40&md5=d60a43d71453323145b2d36ed12754bd.
[30] Lindop JE, Treece GM, Gee AH, Prager RW. 3D elastography using freehand ultrasound. *Ultrasound in Medicine and Biology*. 2006;32(4):529–545.
[31] Yaniv Z, Foroughi P, Kang H-J, Boctor E. Ultrasound calibration framework for the image-guided surgery toolkit (IGSTK). 2011:79641N–79641N–11.
[32] Trobaugh JW, Trobaugh DJ, Richard WD. Three-dimensional imaging with stereotactic ultrasonography. *Computerized Medical Imaging and Graphics*. 1994;18(5):315–323.
[33] Bader W, Böhmer S, Van Leeuwen P, Hackmann J, Westhof G, Hatzmann W. Does texture analysis improve breast ultrasound precision? *Ultrasound in Obstetrics and Gynecology*. 2000;15(4):311–316.
[34] Liao YY, Wu JC, Li CH, Yeh CK. Texture feature analysis for breast ultrasound image enhancement. *Ultrason Imaging*. 2011;33:264–278.
[35] Chen Q, Liu Q. Textural feature analysis for ultrasound breast tumor images. In: *2010 4th International Conference on Bioinformatics and Biomedical Engineering, iCBBE 2010*.; 2010.
[36] Lunn KE, Paulsen KD, Roberts DW, Kennedy FE, Hartov A, Platenik LA. Nonrigid brain registration: Synthesizing full volume deformation fields from model basis solutions constrained by partial volume intraoperative data. *Computer Vision and Image Understanding*. 2003;89(2-3):299–317.
[37] Nakamoto M, Hirayama H, Sato Y, et al. Recovery of respiratory motion and deformation of the liver using laparoscopic freehand 3D ultrasound system. *Medical Image Analysis*. 2007;11(5):429–442.